

RESEARCH

Open Access



# The potential role of T2\*-weighted multi-echo data image combination as an imaging marker for intraplaque hemorrhage in carotid plaque imaging

My Truong<sup>1,2</sup> , Claes Håkansson<sup>1,2</sup> , Makda HaileMichael<sup>1</sup>, Jonas Svensson<sup>1,6</sup>, Jimmy Lätt<sup>1</sup> , Karin Markenroth Bloch<sup>3</sup> , Roger Siemund<sup>1,2</sup> , Isabel Gonçalves<sup>4,5</sup> and Johan Wassélius<sup>1,2,7\*</sup>

## Abstract

**Background:** Carotid atherosclerotic plaques with intraplaque hemorrhage (IPH) are associated with elevated stroke risk. IPH is predominantly imaged based on paramagnetic properties of the *upstream* hemoglobin degradation product methemoglobin. This is an explorative observational study to test the feasibility of a spoiled gradient echo based T2\* weighted MRI sequence (3D MEDIC) for carotid plaque imaging, and to compare signs suggestive of the *downstream* degradation product hemosiderin on 3D MEDIC with signs of methemoglobin on a T1wBB sequence.

**Methods:** Patients with recent TIA or stroke were selected based on the presence on non-calcified plaque components on CTA to promote an enriched prevalence of IPH in the material. Patients (n = 42) underwent 3T MRI with 3D MEDIC and 2D turbo spin echo T1w black blood (T1wBB). Images were independently evaluated by two neuroradiologists and Cohens Kappa was used for inter-reader agreement for each sequence.

**Results:** The technical feasibility for 3D MEDIC, was 34/42 patients (81%). Non-calcified plaque components with susceptibility effect *without* simultaneous T1-shortening—a combination suggestive of hemosiderin, was seen in 13/34 of the plaques. An equally large group display elevated T1w signal *in combination with* signal loss on 3D MEDIC, a combination suggestive of both hemosiderin and methemoglobin. Cohen's kappa for inter-reader agreement was 0.64 (CI 0.345–0.925) for 3D MEDIC and 0.94 (CI 0.81–1.00) for T1wBB.

**Conclusions:** 3D MEDIC shows signal loss, without elevated T1w signal on T1wBB, in non-calcified tissue in many plaques in this group of patients. If further studies, including histological verification, confirm that the 3D MEDIC susceptibility effect is indeed caused by hemosiderin, 3D MEDIC could aid in the detection of IPH, beyond elevation of T1w signal.

**Keywords:** MRI, Atherosclerosis, Carotid plaque, Vessel wall imaging, Intraplaque hemorrhage

## Introduction

Stroke is the leading cause of adult disability and the second leading cause of death worldwide [1]. One major cause of stroke is atherosclerotic plaques in the carotid arteries [2] and the plaque composition is important in the risk assessment. MRI is widely used to assess such

\*Correspondence: Johan.Wasselius@gmail.com

<sup>1</sup> Department of Medical Imaging and Physiology, Skåne University Hospital, Lund, Sweden

Full list of author information is available at the end of the article



plaque characteristics [3–7] as intraplaque hemorrhage (IPH), thin fibrous cap and large necrotic lipid core [3, 4, 8, 9]. IPH is one of the hallmark characteristics of *vulnerable plaques* associated with elevated stroke risk [3, 4, 10–12], also in patients with low grade stenosis [13].

Radiological diagnosis of IPH by MRI relies primarily on the paramagnetic properties of methemoglobin, which is an early degradation product from hemoglobin and the only degradation product with T1 shortening [14, 15]. Methemoglobin is therefore viewed as the major source of elevated T1w signal in tissue [14, 16, 17] and suggestive of relatively *recent* plaque hemorrhage [7, 12, 14, 15]. Identification of the downstream degradation product hemosiderin is appealing as it may be a longer lasting sign of IPH, thereby potentially adding information to the risk assessment of plaques, especially in patients with previous cerebrovascular events.

Hemosiderin has a susceptibility effect due to its supermagnetic properties and Susceptibility Weighted Imaging (SWI) [18–21] has therefore been used to identify hemosiderin or IPH in general [18, 22], but SWI is sensitive to movement artifacts and therefore not ideal for use in the neck region. To our knowledge the relationship of T1w signal and susceptibility effects in non-calcified carotid plaque components, has not been extensively studied. In clinical cervical spinal cord imaging, a spoiled gradient echo-based T2\* weighted sequence called Multi-Echo Data Image Combination (MEDIC, Siemens Healthineers) has been found to be resistant to CSF flow artefacts [23] and to provide good contrast between the grey- and white matter of the spinal cord [24]. These properties could potentially also make it useful to detect hemosiderin in plaques, especially since the 3D MEDIC sequence also allows high spatial resolution.

The aim of this explorative study was to image non-calcified carotid plaque components with 3D MEDIC and compare signs of hemosiderin with elevation of T1w signal in patients with recent TIA or stroke. This population was selected to promote a high prevalence of IPH.

## Material and methods

### Patients

Initial screening for subjects was done by a neuroradiologist (MT) on the basis of CT angiographies (CTA) of the cervical and intracranial arteries between September 2014 and July 2016 at our institution. Patients were considered based on the following inclusion criteria:

1. TIA or ischemic stroke within two weeks of the examination; AND
2. An atherosclerotic carotid plaque with a non-calcified component on the symptomatic side.

Exclusion criteria were:

1. Any contraindications to MRI; OR
2. Atrial fibrillation; OR
3. Internal carotid artery occlusion on the symptomatic side; OR
4. Age below 18 or inability to give informed consent.

The study was approved by the Regional Ethical Review Board and written informed consent was obtained from all included patients.

### CTA protocol

Patients were examined on either of two 64-slice CT scanners (Brilliance 64 and Ingenuity, Philips, Best, The Netherlands). Intravenous iodine The CTA was performed with intravenous Iodine contrast in arterial phase, 12–15 s after administration.

Contrast medium were either 60 ml Iomeron 400 mg/ml (Bracco, Milan, Italy) or 70 ml Omnipaque 350 mg/ml (GE Healthcare, Chicago, USA), and patients were scanned from the aortic arch to the vertex, when the attenuation reached above 200 HU in the internal carotid artery at bolus pre scan.

Reconstructed and stored images: 0.8/0.4 mm (thickness/increment) source images, 3/2 mm. Maximal projection images reconstructions in axial, sagittal and coronary planes.

### Protocol parameters Philips Brilliance 64

Voltage 120 kV, reference exposure 224 mAs. Pitch 0.609, rotation time 0.5 s, collimation 64 × 0.625 mm, slice thickness 0.8 mm, increment 0.4 mm, Acquisition matrix 512 and dose modulation iDose level 3.

### Protocol parameters Philips Ingenuity

Voltage 120 kV, reference exposure 251 mAs, pitch 0.953, rotation time 0.5 s, collimation 64 × 0.625, slice thickness 0.8 mm, increment 0.4 mm, Acquisition matrix 512 and dose modulation iDose level 3.

### MRI protocol

Patients were examined on a 3 T MRI scanner (Magnetom Skyra, Siemens Healthineers, Erlangen, Germany) equipped with a dedicated eight element phased array carotid surface receive coil (Rapid Biomedical Rimpac, Germany).

The clinical protocol included pre- and post- Gadolinium-enhanced acquisitions with a total scan time of 22 min is shown in Table 1 and sequence information for the 2 sequences used in the evaluation is shown in Table 2. The real examination time for each patient however, ranged between 20 and 50 min, depending on the

**Table 1** MRI protocol

Sequence	Time (min)
Localizer	0:13
TOF 3D	4:08
TSE 2D T1wBB	4:30
3D MEDIC	3:54
Gadolinium (Dotarem®) administration + delay*	5:0
TSE 2D T1wBB + Gd*	4:30

Estimated scan times for each sequence of the MRI protocol

\*The post-Gd sequence was not included in this analysis, but part of the clinical MRI protocol

**Table 2** MRI sequence parameters

Sequence parameter	TSE2D T1wBB	3D MEDIC
Acquired in-plane resolution (mm x mm)	0.5 x 0.5	0.7 x 0.7
Reconstructed in-plane resolution (mm x mm)	0.3 x 0.3	0.7 x 0.7
Slice thickness (mm)	2	0.7
Number of slices	15	60
Repetition time, TR (ms)	750	29
Echo time, TE (ms)	10	16
α°	-	8
Number of echoes	-	3
Turbo spin factor	11	-
Time duration (min: s)	4:30	3:54

MRI sequence parameters for the T1wBB and 3D MEDIC sequence

need for re-scans due to patient movement. The two sequences used for evaluation of intraplaque hemorrhage in this study, a fat-saturated 2D Turbo spin echo black blood sequence (T1wBB) and a 3D MEDIC sequence, were both acquired before contrast injection. Patients were in supine position with a pillow as neck support and heads slightly extended and carotid coils bilaterally positioned as close to the carotid bifurcation as possible. In cases where bilateral optimal coil positioning was difficult due to anatomic limitations such as a short neck, the symptomatic side was prioritized. Axial slices for 3D MEDIC and T1wBB were positioned perpendicular to the common carotid artery oriented after a 3D TOF with the following sequence parameters:

T1wBB: Time of acquisition 4:26 min. 15 slices collected sequentially, slice thickness 2.0 mm, distance factor 0%, phase encoding direction A-P, FoV read 160 mm, FoV phase 75%, base resolution 320, phase resolution 100%, voxel size: 0.5 x 0.5 mm<sup>2</sup> interpolated to 0.3 x 0.3 mm<sup>2</sup>, TR=800 ms, TE=10 ms, Turbo factor 11. Fat saturation strong.

3D MEDIC: Time of acquisition 3:54, voxel size: 0.7 x 0.7mm<sup>2</sup>, 60 slices, slice thickness 0,7 mm, slice oversampling 6.7%, phase encoding direction A-P, FoV 180 mm, FoV phase 100%, base resolution 256, phase resolution 100%, TR=29 ms, TE=16,0 ms, 3 echoes, Flip angle 8°, Fat suppression: Water excitation normal.

**Image analysis**

All images were independently reviewed by two experienced neuroradiologists (MT and CH) (SECTRA PACS IDS7, Sectra AB, Linköping, Sweden) on dedicated high-resolution image working stations (Barco medical screens model MDCC-6430, Kortrijk, Belgium). In cases with disagreement between the observers, a consensus decision was reached, that was used for the analysis. Inter-rater agreement was calculated using Cohen’s kappa with a 95% confidence interval.

The co-localization analysis was done visually, on trans-axial CTA and MR images (3D MEDIC and T1wBB) side by side. The images were synchronized based on distinct morphologic landmarks such as macro-calcifications, plaque shape and the bifurcation. The matching of levels and synchronization of the three stacks was done by one of the reviewers and the settings were saved to ensure that both reviewers analyzed the same matched levels.

Areas within the plaque, were labelled as *non-calcified plaque components*, if the attenuation on CTA images was between 0-200HU and labelled as *calcifications* if the plaque attenuation was 500–1000 HU on CTA. Degree of stenosis on MRI and CTA was calculated by the common carotid artery method [25].

If the vessel contained more than one non-calcified plaque component, the largest was selected.

*Signal loss on 3D MEDIC* was defined as any area within a non-calcified plaque component with signal intensity lower than the ipsilateral sternocleidomastoid muscle. In cases of uncertainty, the signal in the plaque was measured within a circular ROI and compared to the measured signal value of a ROI placed in the muscle. If the signal difference was more than 1.5 times, we decided that the signal loss was significant. The classification of signal loss was binary and labeled *MEDIC+* if signal loss was seen and *MEDIC-* if signal loss was absent.

*Elevation of T1w signal* was defined as higher signal within the plaque component than in the ipsilateral sternocleidomastoid muscle and the common carotid artery on the T1wBB images.

In cases of uncertainty, the signal in the plaque was measured with a ROI tool and compared to the measured

**Table 3** Patient data

All patients with complete imaging (n)	34
Median age (total range, IQR)	72.5 (35–86, 66–78)
Female (%)	11 (32)
Indication	
TIA n (%)	11 (32)
Stroke n (%)	23 (68)
Degree of stenosis %	
CTA median (total range, IQR)	70 (35–95, 50–88)
MRI median (total range, IQR)	70 (35–95, 60–88)

Demographic data for the 34 patients with a full set of diagnostic images

**Table 4** The distribution of signal loss on 3D MEDIC and elevated T1w signal on the T1wBB

	Signal loss 3D MEDIC +	No signal loss 3D MEDIC -	
T1w +	13/34 (38%)	1/34 (3%)	14/34 (41%)
T1w -	13/34 (38%)	7/34 (21%)	20/34 (59%)
	26/34 (76%)	8/34 (24%)	

Cross table with the distribution of the presence or absence of signal loss on 3D MEDIC and T1w signal elevation in the 34 plaques. The four groups have the same color representation as used in Fig. 1

signal value found in the muscle. If the signal difference was more than 1.5 times, we decided that the elevated signal on T1wBB, was significant. The classification was binary and labelled *T1wBB+* if elevated T1w signal was seen and *T1wBB-* if absent.

## Results

### Patient population

Between September 2014 and July 2016, 1280 consecutive CTA were screened for candidates, and the 46 patients that met all inclusion criteria were considered for inclusion. Four of these had contraindications to MRI that were not known at inclusion or withdrew from participation after the initial consent.

Of the 42 patients that completed the MRI examination, 3D MEDIC images were non-diagnostic, typically due to patient motion in 8 patients, resulting in 34 patients with a full set of diagnostic images for the final image analysis (Table 3).

### Image analysis

The results of the image analysis are shown in Table 4 and the corresponding typical patterns are illustrated in Fig. 1.

The column **3D MEDIC +** represents signal loss on 3D MEDIC. The row **T1w +** represents presence of T1w signal elevation on T1wBB.

The blue box in Table 4 shows the proportion of plaques n (%) with signal loss on 3D MEDIC and elevated T1w signal on T1wBB. The green box indicates the proportion of plaques with signal loss without elevated T1w signal. The white box indicates the proportion of plaques without signal loss and no elevation of T1w signal. The Yellow box show the one plaque with elevated T1w signal without signal loss on 3D MEDIC.

The median degree of stenosis, calculated by the common carotid artery method, was 70% on CTA (IQR = 50–88%) as well as on MRI (IQR = 60–88%).

All areas with macro-calcifications on CTA showed corresponding signal loss on 3D MEDIC. The majority of plaques (26/34, 76%) had signal loss within the non-calcified component, suggestive of the presence of hemosiderin, on 3D MEDIC. Less than half of the plaques 14/34 (41%) had an elevated T1wBB signal within the non-calcified component, suggestive of the presence of methemoglobin.

Cohen’s kappa for inter-reader agreement was 0.64 (CI 0.345–0.925) for 3D MEDIC and 0.94 (CI 0.81–1.00) for T1wBB.

## Discussion

This is an explorative observational study to test the feasibility of a spoiled gradient echo based T2\* weighted MRI sequence (3D MEDIC) for carotid plaque imaging, and to compare signs suggestive of hemosiderin on 3D MEDIC with signs of methemoglobin on a T1wBB sequence.

The patients were selected based on the presence on non-calcified plaque components on CTA and with recent TIA or stroke. This designed selection bias was intended to promote an enriched prevalence of IPH in the material.

The anatomy of the common carotid was often asymmetric, both in terms of angle but often also not exactly symmetrical in level. Correct coil placement was very important. The closer the coil was to the vessel, the better was SNR and CNR (visually assessed). We always aimed at acquiring high-quality scan of both sides but in situations when the patient had a short neck, the symptomatic side was prioritized and the patient would have to tilt the head slightly to the contralateral side for the surface coil to fit on the symptomatic side. This set some limitations with sometimes suboptimal coil placement on the non-symptomatic side.

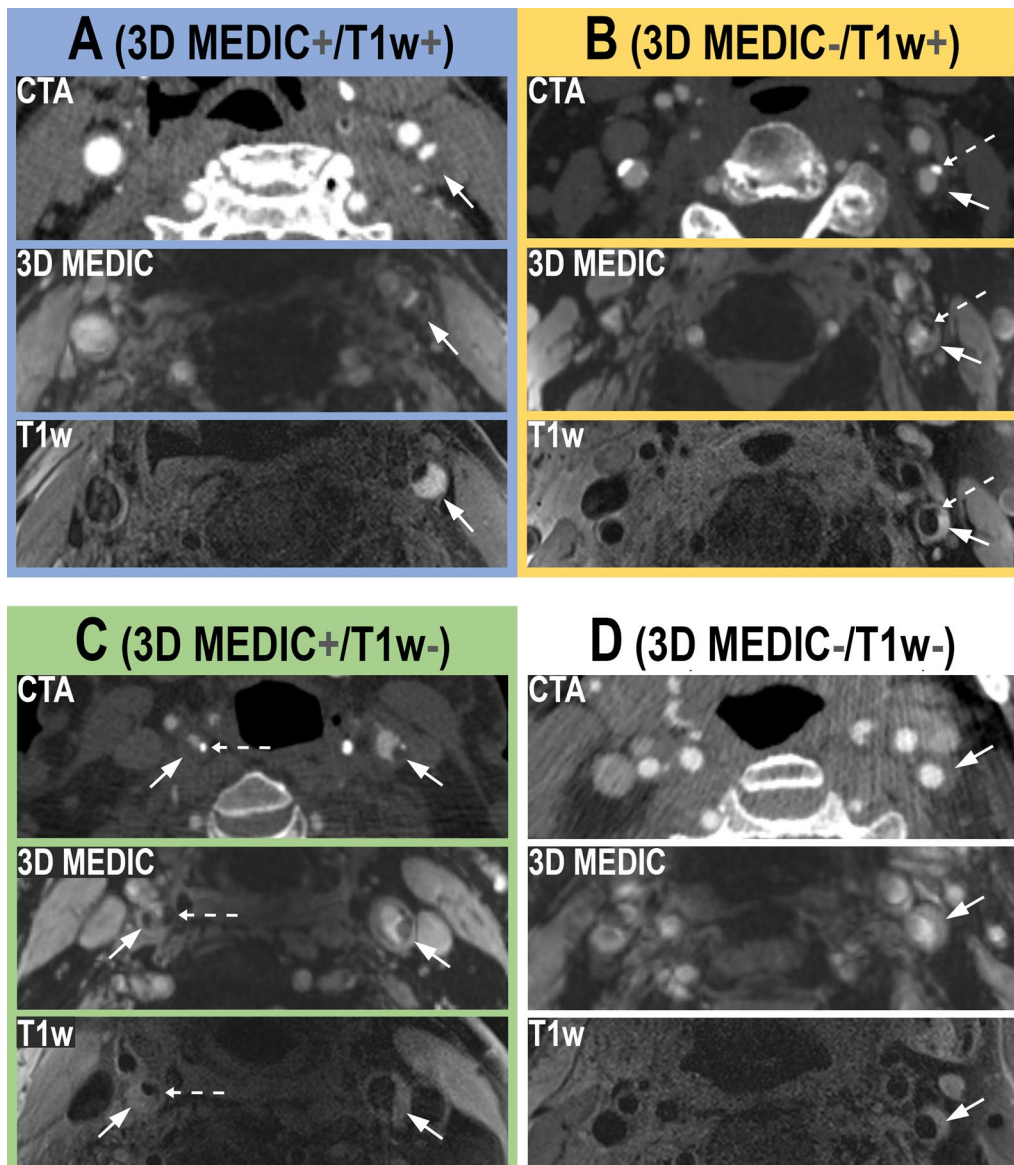


**Fig. 1** Typical imaging findings for each of the four groups at the level of the carotid bifurcation on CTA, 3D MEDIC and T1wBB, described in Table 4. The color representation for each of the four groups are the same as in Table 4. In panel **A**, in blue color, the arrow indicates a large non-calcified plaque component with signal loss on 3D MEDIC and elevated T1w signal (**3DMEDIC +/T1w +**). In panel **B**, in yellow color, the arrow indicates a non-calcified plaque component with no signal loss on 3D MEDIC and elevated T1w signal (**3DMEDIC-/T1w +**). The dotted arrow indicates a calcification, with high attenuation on CTA, signal loss on 3D MEDIC and signal loss on T1w. In panel **C**, in green color, the filled arrows on both sides indicate large non-calcified plaque components with signal loss on 3D MEDIC and no elevation of T1w signal (**MEDIC +/T1w -**). The dotted arrow on the left side indicate a calcification, with high attenuation on CTA, signal loss on 3D MEDIC and signal loss on T1w on the asymptomatic side (this side was not included in final image analysis). In panel **D**, in white color, the arrow indicates a small non-calcified plaque without signal loss on 3D MEDIC and no T1w signal elevation (**MEDIC-/T1w -**)

During planning of the axial slices of the 3D MEDIC and the T1wBB, the vessel on the symptomatic side, seen on the TOF sequence, was used to set the axial slices perpendicular to the common carotid artery. This could affect the result with a slightly oblique slice plane of the T1wBB images on the non-symptomatic side. This was

less of a problem for the 3D MEDIC, which was volumetric, and could be reconstructed in MPR.

The degree of technical feasibility for 3D MEDIC, defined as images acceptable to both neuroradiologist readers, was 34/42 patients (81%). The poorer inter-reader agreement for 3D MEDIC compared to T1wBB

may suggest that the image quality was inferior for the 3D MEDIC, even though the images were accepted by both readers. There are other possible explanations for the lower inter-reader agreement, such as lesser experience of 3D MEDIC images.

In atherosclerotic plaques with IPH, different hemoglobin degradation products are known to co-localize [26]. Intracellular methemoglobin, extracellular methemoglobin and hemosiderin affects the signal characteristics on MRI differently [14], and if the degradation products of hemoglobin co-localize, the MRI image can become complex and IPH diagnosis difficult to make. Simpson et al. [27] showed in a study with 37 patients, that the elevated T1w signal was visible for 2 years in the majority of cases.

By applying the 3D MEDIC sequence together with a T1wBB sequence, we show that non-calcified plaques contain tissue that affects susceptibility *without* simultaneous T1-shortening and that this is in fact a relatively common imaging feature present in 13/34 of the plaques in this group of patients. This image features would be suggestive of hemosiderin with little or no methemoglobin. Our study also shows that an equally large group display elevated T1w signal *in combination with* signal loss on 3D MEDIC (Table 4 and Fig. 1), an imaging feature suggestive of hemosiderin and methemoglobin in combination. An alternative explanation for this finding could be the presence of very small amounts of calcium, undetectable on CTA, which have also been demonstrated within atherosclerotic plaques [11]. A recent study by Wang et al. [21] showed co-localization of elevated T1w signal and susceptibility artefacts, similar to our finding, as well as the capability of quantitative susceptibility mapping to discern macro-calcifications from hemorrhage.

In 7/34 of the examined plaques in our study no signal loss on 3D MEDIC or T1w-elevation was seen, which may indicate a more stable plaque composition. Lastly, we found that elevated T1w signal *without* signal loss on 3D MEDIC was an uncommon finding in this group of patients, only seen in one plaque in our study.

There are several limitations of this study. There was no histological or biochemical verification of the imaging findings, which would eventually be desired to support the hypothesis that 3D MEDIC can be used to identify hemosiderin. This was not possible since only a small portion of the included patients were treated surgically. Another limitation is that a SWI sequence was not included in the imaging protocol. This would be desirable to compare the technical feasibility with 3D MEDIC. In our experience successful high-resolution SWI imaging of carotid plaques in 34 out of 42

patients would be challenging with SWI sequences, but this remains to be further studied.

## Conclusion

This study show that high-resolution plaque imaging using 3D MEDIC is feasible in the large majority of patients, and that the properties of the sequences used here theoretically may separately identify the different hemoglobin degradation products methemoglobin and hemosiderin, thereby potentially adding information of IPH and prolonging the period when IPH can be visualized on MRI.

## Abbreviations

CI: Confidence interval; CSF: Cerebrospinal fluid; CTA: Computed tomography angiography; FoV: Field of view; Gd: Gadolinium; HU: Hounsfield unit; ICA: Internal carotid artery; IPH: Intra plaque hemorrhage; IQR: Interquartile range; MEDIC: Multi-Echo Data Image combination; MRI: Magnetic resonance imaging; ms: Millisecond; PACS: Picture Archiving and Communication System; SPGR: Spoiled gradient echo; SWI: Susceptibility weighted imaging; TE: Time of echo; TIA: Transient ischemic attack; TOF 3D: Time of flight in 3D; TR: Repetition time; TSE2D T1wBB: Turbo spin echo 2D T1 weighted black blood; T2\*: T2 star;  $\alpha^\circ$ : Flip angle.

## Acknowledgements

Dr. Lee Nolan is gratefully acknowledged for professional language editing. Professor Peter Höglund is gratefully acknowledged for professional statistical expertise. Johanna Arborelius, Siv Tjernberg and Amir Vahabi are gratefully acknowledged as MRI technicians.

## Authors' contributions

All authors contributed to the study conception and design. Material preparation and data collection were performed by MT and MHM. MRI protocol was set up by MT, JS, JL and KMB. The image analysis was performed by MT and CH. The first draft of the manuscript was written by MT and JW and all authors commented on the manuscript. All authors read and approved the final manuscript.

## Funding

Open access funding provided by Lund University. This work was supported by The Olle Olsson foundation and The Swedish Society of Radiology to MT, by the Crafoord Foundation (#20180610), STINT (The Swedish Foundation for International Cooperation in Research and Higher Education #B2018-7532), The Swedish Stroke Association, Skåne University Hospital and Region Skåne (I-ALF 47447 and YF-ALF 43435) to JW, and by the Swedish Research Council, Swedish Heart and Lung Foundation and Skåne University Hospital funds to IG.

## Availability of data and materials

The data that support the findings of this study are available from the corresponding author, upon reasonable request.

## Code availability

Not applicable.

## Declarations

### Ethics approval and consent to participate

All procedures performed in the studies involving human participants were in accordance with the ethical standards of the regional research committee and with the 1964 Helsinki Declaration and its later amendments or comparable ethical standards. Approval was granted by the Regional Ethical Review Board of Lund University.

**Consent for publication**

Written informed consent was obtained from all individual participants included in the study. NA for consent to publication.

**Competing interests**

The authors declare that they have no competing interests.

**Author details**

<sup>1</sup>Department of Medical Imaging and Physiology, Skåne University Hospital, Lund, Sweden. <sup>2</sup>Department of Clinical Sciences, Lund University, Lund, Sweden. <sup>3</sup>Lund University Bioimaging Centre, Lund University, Lund, Sweden. <sup>4</sup>Department of Clinical Sciences, Lund University, Malmö, Sweden. <sup>5</sup>Department of Cardiology, Skåne University Hospital, Malmö, Sweden. <sup>6</sup>Medical Radiation Physics, Department of Translational Medicine, Lund University, Lund, Sweden. <sup>7</sup>Department of Radiology, Skåne University Hospital, 221 85 Lund, Sweden.

Received: 3 March 2021 Accepted: 14 July 2021

Published online: 11 August 2021

**References**

1. Feigin VL, Norrving B, Mensah GA. Global burden of stroke. *Circ Res*. 2017;120(3):439–48. <https://doi.org/10.1161/circresaha.116.308413>.
2. Libby P, Buring JE, Badimon L, Hansson GK, Deanfield J, Bittencourt MS, Tokgozoglul L, Lewis EF. Atherosclerosis. *Nat Rev Dis Primers*. 2019;5(1):56. <https://doi.org/10.1038/s41572-019-0106-z>.
3. Hosseini AA, Kandiyil N, MacSweeney ST, Altaf N, Auer DP. Carotid plaque hemorrhage on magnetic resonance imaging strongly predicts recurrent ischemia and stroke. *Ann Neurol*. 2013;73(6):774–84. <https://doi.org/10.1002/ana.23876>.
4. Hosseini AA, Simpson RJ, Altaf N, Bath PM, MacSweeney ST, Auer DP. Magnetic resonance imaging plaque hemorrhage for risk stratification in carotid artery disease with moderate risk under current medical therapy. *Stroke*. 2017;48(3):678–85. <https://doi.org/10.1161/strokeaha.116.015504>.
5. Yuan C, Kerwin WS, Ferguson MS, Polissar N, Zhang S, Cai J, Hatsukami TS. Contrast-enhanced high resolution MRI for atherosclerotic carotid artery tissue characterization. *J Magn Reson Imaging JMRI*. 2002;15(1):62–7.
6. Cai J, Hatsukami TS, Ferguson MS, Kerwin WS, Saam T, Chu B, Takaya N, Polissar NL, Yuan C. In vivo quantitative measurement of intact fibrous cap and lipid-rich necrotic core size in atherosclerotic carotid plaque: comparison of high-resolution, contrast-enhanced magnetic resonance imaging and histology. *Circulation*. 2005;112(22):3437–44. <https://doi.org/10.1161/CIRCULATIONAHA.104.528174>.
7. Cai JM, Hatsukami TS, Ferguson MS, Small R, Polissar NL, Yuan C. Classification of human carotid atherosclerotic lesions with in vivo multicontrast magnetic resonance imaging. *Circulation*. 2002;106(11):1368–73.
8. Moody AR, Singh N. Incorporating carotid plaque imaging into routine clinical carotid magnetic resonance angiography. *Neuroimaging Clin N Am*. 2016;26(1):29–44. <https://doi.org/10.1016/j.nic.2015.09.003>.
9. Kerwin WS. Carotid artery disease and stroke: assessing risk with vessel wall MRI. *ISRN Cardiol*. 2012;2012: 180710. <https://doi.org/10.5402/2012/180710>.
10. Saam T, Hetterich H, Hoffmann V, Yuan C, Dichgans M, Poppert H, Koepfel T, Hoffmann U, Reiser MF, Bamberg F. Meta-analysis and systematic review of the predictive value of carotid plaque hemorrhage on cerebrovascular events by magnetic resonance imaging. *J Am Coll Cardiol*. 2013;62(12):1081–91. <https://doi.org/10.1016/j.jacc.2013.06.015>.
11. Redgrave JN, Lovett JK, Gallagher PJ, Rothwell PM. Histological assessment of 526 symptomatic carotid plaques in relation to the nature and timing of ischemic symptoms: the Oxford plaque study. *Circulation*. 2006;113(19):2320–8. <https://doi.org/10.1161/circulationaha.105.589044>.
12. Michel JB, Virmani R, Arbustini E, Pasterkamp G. Intraplaque haemorrhages as the trigger of plaque vulnerability. *Eur Heart J*. 2011;32(16):1977–85. <https://doi.org/10.1093/eurheartj/ehr054>.
13. Yoshida K, Sadamasa N, Narumi O, Chin M, Yamagata S, Miyamoto S. Symptomatic low-grade carotid stenosis with intraplaque hemorrhage and expansive arterial remodeling is associated with a high relapse rate refractory to medical treatment. *Neurosurgery*. 2012;70(5):1143–50.

<https://doi.org/10.1227/NEU.0b013e31823fe50b> (discussion 1141–1150).

14. Bradley WG Jr. MR appearance of hemorrhage in the brain. *Radiology*. 1993;189(1):15–26. <https://doi.org/10.1148/radiology.189.1.8372185>.
15. Bass J, Sostman HD, Boyko O, Koepke JA. Effects of cell membrane disruption on the relaxation rates of blood and clot with various methemoglobin concentrations. *Investig Radiol*. 1990;25(11):1232–7.
16. Zizka J, Elias P, Hodik K, Tintera J, Juttnerova V, Belobradek Z, Klzo L. Liver, meconium, haemorrhage: the value of T1-weighted images in fetal MRI. *Pediatr Radiol*. 2006;36(8):792–801. <https://doi.org/10.1007/s00247-006-0239-6>.
17. Flores DV, Mejía Gómez C, Estrada-Castrillón M, Smitaman E, Pathria MN. MR imaging of muscle trauma: anatomy, biomechanics, pathophysiology, and imaging appearance. *Radiographics*. 2018;38(1):124–48. <https://doi.org/10.1148/rg.2018170072>.
18. Liu S, Buch S, Chen Y, Choi HS, Dai Y, Habib C, Hu J, Jung JY, Luo Y, Utrianen D, Wang M, Wu D, Xia S, Haacke EM. Susceptibility-weighted imaging: current status and future directions. *NMR Biomed*. 2017;30(4):e3552. <https://doi.org/10.1002/nbm.3552>.
19. Yang Q, Liu J, Barnes SR, Wu Z, Li K, Neelavalli J, Hu J, Haacke EM. Imaging the vessel wall in major peripheral arteries using susceptibility-weighted imaging. *J Magn Reson Imaging JMRI*. 2009;30(2):357–65. <https://doi.org/10.1002/jmri.21859>.
20. Barnes SR, Haacke EM. Susceptibility-weighted imaging: clinical angiographic applications. *Magn Reson Imaging Clin N Am*. 2009;17(1):47–61. <https://doi.org/10.1016/j.mric.2008.12.002>.
21. Wang C, Zhang Y, Du J, Huszar IN, Liu S, Chen Y, Buch S, Wu F, Liu Y, Jenkinson M, Hsu CC, Fan Z, Haacke EM, Yang Q. Quantitative susceptibility mapping for characterization of intraplaque hemorrhage and calcification in carotid atherosclerotic disease. *J Magn Reson Imaging JMRI*. 2020. <https://doi.org/10.1002/jmri.27064>.
22. Liu Q, Fan Z, Yang Q, Li D. Peripheral arterial wall imaging using contrast-enhanced, susceptibility-weighted phase imaging. *J Comput Assist Tomogr*. 2012;36(1):77–82. <https://doi.org/10.1097/RCT.0b013e3182388cdf>.
23. Martin N, Malfair D, Zhao Y, Li D, Traboulssee A, Lang D, Vertinsky AT. Comparison of MERGE and axial T2-weighted fast spin-echo sequences for detection of multiple sclerosis lesions in the cervical spinal cord. *AJR Am J Roentgenol*. 2012;199(1):157–62. <https://doi.org/10.2214/ajr.11.7039>.
24. Benjamin EJ, Virani SS, Callaway CW, Chamberlain AM, Chang AR, Cheng S, Chiuve SE, Cushman M, Dellinger FN, Deo R, de Ferranti SD, Ferguson JF, Fornage M, Gillespie C, Isasi CR, Jimenez MC, Jordan LC, Judd SE, Lackland D, Lichtman JH, Lisabeth L, Liu S, Longenecker CT, Lutsey PL, Mackey JS, Matchar DB, Matsushita K, Mussolino ME, Nasir K, O'Flaherty M, Palaniappan LP, Pandey A, Pandey DK, Reeves MJ, Ritchey MD, Rodriguez CJ, Roth GA, Rosamond WD, Sampson UKA, Satou GM, Shah SH, Spartano NL, Tirschwell DL, Tsao CW, Voeks JH, Willey JZ, Wilkins JT, Wu JH, Alger HM, Wong SS, Muntner P. Heart disease and stroke statistics-2018 update: a report from the American Heart Association. *Circulation*. 2018;137(12):e67–492. <https://doi.org/10.1161/cir.0000000000000558>.
25. Rothwell PM, Gibson RJ, Slattery J, Sellar RJ, Warlow CP. Equivalence of measurements of carotid stenosis. A comparison of three methods on 1001 angiograms. *European Carotid Surgery Trialists' Collaborative Group. Stroke*. 1994;25(12):2435–9. <https://doi.org/10.1161/01.str.25.12.2435>.
26. Derksen WJ, Peeters W, van Lammeren GW, Tersteeg C, de Vries JP, de Kleijn DP, Moll FL, van der Wal AC, Pasterkamp G, Vink A. Different stages of intraplaque hemorrhage are associated with different plaque phenotypes: a large histopathological study in 794 carotid and 276 femoral endarterectomy specimens. *Atherosclerosis*. 2011;218(2):369–77. <https://doi.org/10.1016/j.atherosclerosis.2011.07.104>.
27. Simpson RJ, Akwei S, Hosseini AA, MacSweeney ST, Auer DP, Altaf N. MR imaging-detected carotid plaque hemorrhage is stable for 2 years and a marker for stenosis progression. *AJNR Am J Neuroradiol*. 2015;36(6):1171–5. <https://doi.org/10.3174/ajnr.A4267>.

**Publisher's Note**

Springer Nature remains neutral with regard to jurisdictional claims in published maps and institutional affiliations.